Predictions of nitrogen isotropic hyperfine coupling constants in the nitroxide radicals with the aid of DF/HF calculations

A. Zakrassov and M. Kaftory*

Lise Meitner Minerva Center for the Computational and Quantum Chemistry, Department of Chemistry, Technion—Israel Institute of Technology, Haifa 32000, Israel

Abstract

Nitrogen isotropic hyperfine coupling constants in different nitroxide radicals calculated via ab initio hybrid density functional/Hartree–Fock methods (UB3LYP and UB1LYP) with 6-31G(d) basis set of Gaussian 98 were found to be in a good agreement with the experimental EPR results. UB3LYP/6-31G(d) and UBLYP/6-31G(d) calculated atomic spin populations and spin density maps in the gas phase correspond to the general features of the experimentally obtained data by polarized neutron diffraction studies in the solid state. The results were analyzed in terms of unpaired electron delocalization and the influence of the surrounding on the radical centers.

© 2002 Elsevier Science (USA). All rights reserved.

1. Introduction

The possibility of ferromagnetic coupling in organic radicals was theoretically predicted in 1963 by McConnell [1]. Since the discovery in 1991 by Kinoshita and coworkers [2], the bulk ferromagnetic behavior at 0.65 K of pure organic radical *p*-nitrophenyl nitronyl nitroxide radical (*β*-phase), there has been an increase of syntheses and investigations of stable organic radicals. The highest Neel temperature obtained so far for pure organic radicals belongs to the *β*-phase of dithiadiazolyl radical, *p*-NCC$_6$F$_4$CNSSN$^•$ exhibiting non-colinear antiferromagnetism at 35.5 K [3].

Ferro or antiferromagnetic coupling of stable radicals depends on the spin density of each atom and the interactions between them [4]. Since no correlation was found between relative orientation of O–N=C–N–O$^•$ groups and the types of coupling [5,6], it seems that ferro or antiferromagnetic coupling in the nitronyl nitroxide radicals is dependent on the shortest contacts between atoms and their spin densities. For example,

ferromagnetic coupling in the different *p*-nitrophenyl nitronyl nitroxide radicals is attributed to the interactions between the aromatic rings [2,7]. The dependence of the spin density distribution on the type of substituents in a large family of nitronyl nitroxide radicals has been investigated by Novoa and co-workers [8]. In the present work, the dependence of the spin density distribution and isotropic hyperfine coupling constants (hfcc) on the type of substituents in different classes of nitroxide radicals is discussed.

Polarized neutron diffraction (PND) studies reveal atomic spin density maps, but the experiments are very expensive and limited by the crystal size. EPR spectra can provide the atomic spin density distribution obtained from isotropic hfcc's of the corresponding nucleus.

The isotropic hfcc's derived from gas phase atomic spin densities, calculated by hybrid density functional/Hartree–Fock (DF/HF) methods, might be a useful tool to predict and explain the ferro or antiferromagnetic coupling of radicals.

The aim is to design ferromagnetically coupled radicals with the aid of DF/HF calculations using Gaussian 98.

*Corresponding author. Fax: +4823-3735.
E-mail address: kaftory@tx.technion.ac.il (M. Kaftory).

2. Methods

The unrestricted B3LYP method (self-consistent hybrid DF/HF approach [9], obtained by the combination of HF and Becke exchange [10,11] with the Lee et al. correlation functional [12]) with 6-31 G(d) basis set of Gaussian 98 has been used for the optimization of the radicals molecular geometry and for the calculations of the atomic spin densities and isotropic hfcc. Also, we have used single point UB1LYP and pure density functional UBLYP calculations with 6-31 G(d) basis set, based on the optimized geometries, to compare the results.

The adiabatic connection formula [13] for the B3LYP method is given as follows:

$$E_{xc}(B3LYP) = a_{x0}E_x(LSD) + (1 - a_{x0})E_x(HF)$$
$$+ a_{x1}\Delta E_x(B) + (1 - a_c)E_c(LSD)$$
$$+ a_c E_c(LYP), \qquad (1)$$

where E_{xc} is the energy of exchange and correlation for electron–electron interactions, $E_x(LSD)$ is the local spin density (LSD) approximation to exchange and correlation, $E_x(HF)$ is the HF exchange energy, $E_x(B)$ is the Becke exchange functional [11] and $E_c(LYP)$ is the Lee et al. correlation functional [12]. The three semiemperical constants were determined by Beck: $a_{x0} = 0.80$, $a_{x1} = 0.72$ and $a_c = 0.81$ [14].

In case of B1LYP Eq. (2) is being used:

$$E_{xc}(B1LYP) = a_0 E_x(HF) + (1 - a_0)(E_x(UEG)$$
$$+ \Delta E_x(B)) + E_c(LYP), \qquad (2)$$

where a_0 is 0.25 as obtained by the analysis of Perdew and co-workers [15].

The nuclear spin density and isotropic hfcc are related by the following equation: [16]

$$a_N = 8\pi g_e \beta_e g_N \beta_N \sum_{\mu,\eta} P^{\alpha-\beta}_{\mu,\eta} < \varphi_\mu[\delta(r_{kN})]\varphi_v > /3h, \qquad (3)$$

where g_e, g_N are the magnetogyric ratios for electron and nuclear, respectively, β_e, β_N are the electron and nuclear magneton, $P^{\alpha-\beta}$ is the difference between the density matrices for electrons with α and β spin, $\delta(r)$ is the Dirac delta operator and h the Planck constant.

Gaussian 98 package reveals Mulliken atomic spin populations of a radical in Bohr magneton units (μ_B) (1 μ_B for doublet ground state, 2 μ_B for triplet ground state, etc.) and Fermi contact analysis representing the computed hfcc's results in miliTesla units (mT). We converted the miliTesla units into Gauss units (G) to enable the comparison with experimental hfcc's data that are usually given in Gauss (1 G = 0.1 mT = 2.8025 MHz).

3. Results and discussion

The optimized radical molecular geometries have been calculated and found to be in a good agreement with the experimental crystallographic data for the same compounds. The compounds for which the calculations have been performed are shown in Fig. 1. The comparison between the calculated and the experimental N–O distances is given in Table 1.

According to PND and EPR studies, the spin densities of nitronyl nitroxide radicals are mainly delocalized on O–N=C–N–O$^\bullet$ fragment. The range of the experimental spin densities on these fragments are from 0.199 [27] (at $T = 5$ K and applied magnetic field $H = 8$ T) to 0.225 [28] (at $T = 4.75$ K and applied magnetic field $H = 8$ T) for the nitrogen, from 0.186 [28] to 0.258 [28] for the oxygen atom and from -0.071 [28] to -0.099 [29] for the α-carbon in PND studies in μ_B units. If the data are scaled to yield 1 μ_B per molecule, the average experimental values for the two NO groups within each of the two molecules are found to be 0.27 μ_B for both nitrogen and oxygen and -0.11 μ_B for α-carbon [28]. The spin densities on the other atoms were found to be in a range of $\pm 10^{-2}$–10^{-3} μ_B [27–29]. The range of the measured total spin density per nitronyl nitroxide molecule in PND studies is from 0.752 μ_B [27] to 0.928 μ_B [28].

The calculated Mulliken atomic spin populations of nitronyl nitroxide radicals (Table 1) are close to experimentally obtained results from PND studies [27–29] and solid state NMR data [30] for the similar compounds. The calculated spin densities of the different nitronyl nitroxide radicals are mostly spreaded on O–N=C–N–O$^\bullet$ fragment in the molecules. We have obtained negative atomic spin densities for the carbon atoms in the 1,3,5 positions (-0.01 to -0.05 μ_B) and positive spin densities for the carbon atoms in the 2,4,6 positions (0.01–0.05 μ_B) in the pyridine and the phenyl ring, similar to the experimental data [27–29]. The calculated spin densities on the other atoms reproduce qualitatively the experimental results ($\pm 10^{-2}$–10^{-3} μ_B [27–29]). The UB3LYP calculated nitrogen spin density of nitronyl nitroxides radicals groups lie in a range of 0.26–0.28 μ_B. This is in excellent agreement with the experimental normalized values of 0.27 μ_B [27]. On the other hand, the UB3LYP calculated spin densities of the radical oxygen (0.34–0.36 μ_B) do not agree with the experimental values of 0.27 μ_B [27].

The spin densities of the α-carbon atom on O–N=C–N–O$^\bullet$ fragment for the nitronyl nitroxide radicals (1–7,11–14) have been calculated to be from -0.24 (1) to -0.195 μ_B (5) (-0.11 μ_B experimental [27]) and for the planar nitroxide radicals (8–10) from -0.16 to -0.18 μ_B (see Table 1). Similar spin densities were obtained by Novoa and co-workers [8] using B3LYP method with different basis sets (6-31 G(d), cc-pVDZ, cc-pCVDZ,
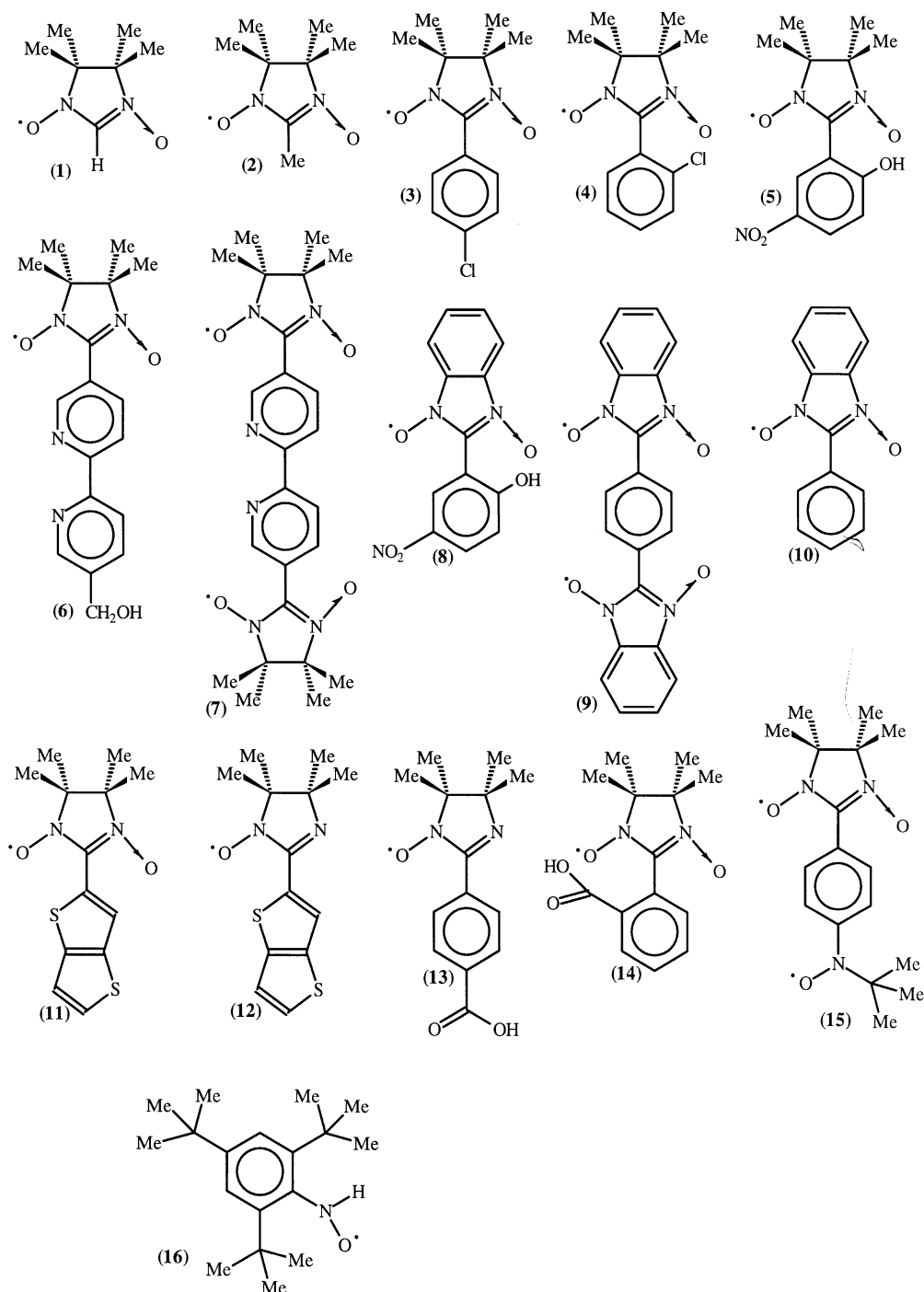
Fig. 1. The compounds used for calculations. **1–5** are compounds prepared, crystallized and X-ray structurally characterized in the present work, **6–9** have also been synthesized, but not structurally characterized.

EPR-II and IGLO-III) for a large family of nitronyl nitroxides.

UBLYP/6-31 G(d) calculations show a decrease of the spin densities by $0.05 \mu_B$ and UB1LYP/6-31 G(d) calculations overestimate the calculated spin densities by more than $0.05 \mu_B$ compared to those calculated by UB3LYP/6-31 G(d) and those experimentally measured. The overestimation of the calculated spin densities by UHF-based methods has been discussed by Yamanaka and co-workers to be a result of spin contamination effects [31]. Nevertheless, UHF-based methods have been found to be applicable to the calculations of the spin densities of organic radicals [31].

Table 1
Spin densities p_s (Bohr magneton μ_B) on O–N=C–N–O$^{\bullet}$ fragment nitrogen hfcc a_N (Gauss) and NO distances d (Å) of the calculated compounds

Compound	p_s (μ_B) (B3LYP)			p_s (μ_B) (BLYP)			a_N (G) (B3LYP)	a_N (G) (B1LYP)	a_N (G) (exp[a])	d (Å) (calc.)	d (Å) (exp.)
	N	O	C	N	O	C					
1[b]	0.26	0.35	−0.24	0.23	0.32	−0.21	5.97	6.70	7.22 [17]	1.27	1.27–1.28[c]
	0.26	0.35		0.23	0.32		5.97	6.70	7.22	1.28	1.28–1.29
2	0.27	0.34	−0.22	0.24	0.32	−0.20	6.18	7.00	7.4 [18]	1.28	1.28[c]
	0.27	0.35		0.24	0.33		6.14	6.96	7.4	1.28	1.28
3[b]	0.28	0.35	−0.22	0.24	0.31	−0.19	6.47	7.27	7.4[d] [19]	1.28	1.28[c]
	0.28	0.35		0.24	0.31		6.47	7.10	7.4	1.28	1.28
4[b]	0.27	0.35	−0.23	0.24	0.32	−0.21	6.48	7.27	7.26 [19]	1.27	1.29[c]
	0.26	0.36		0.22	0.33		5.97	6.78	7.26	1.27	1.27
5[b]	0.28	0.42	−0.195	0.24	0.37	−0.15	6.52	7.46	7.81 [19][d]	1.29	1.32[c]
	0.27	0.23		0.23	0.23		6.60	7.30	7.40	1.27	1.29
6[b]	0.28	0.35	−0.22	0.24	0.32	−0.19	6.60	7.39	—	1.28	—
	0.27	0.36		0.24	0.33		6.46	7.24	—	1.27	—
7[b]	0.28	0.35	−0.22	0.24	0.32	−0.19	3.28	3.72	3.8[6] [20]	1.28	1.28 [20]
	0.27	0.36		0.24	0.32		3.21	3.64	3.8	1.275	1.275
8	0.20	0.46	−0.16	0.17	0.40	−0.13	3.74	4.27	4.1[c]	1.27	—
	0.17	0.23		0.14	0.23		3.59	4.15	4.1	1.29	—
9	0.18	0.37	−0.18	0.16	0.33	−0.15	1.73	2.06	—	1.27	—
	0.18	0.37		0.16	0.33		1.73	2.06	—	1.27	—
10	0.18	0.37	−0.19	0.15	0.34	−0.16	3.63	4.24	4.38 [21]	1.275	1.28 [22]
	0.18	0.37		0.15	0.34		3.63	4.24	4.38	1.275	1.275
11	0.28	0.36	−0.21	0.24	0.33	−0.18	6.7	7.44	7.0 [23]	1.28	1.28 [23]
	0.27	0.35		0.23	0.31		6.62	7.42	7.0	1.28	1.28
12	0.3		−0.11	0.28		−0.09	5.26	5.48	4.5 [23]		
	0.34	0.49		0.32	0.45		7.87	7.35	8.9	1.27	1.26 [23]
13	0.31		−0.12	0.29		−0.10	5.32	5.76	4.28 [24]		
	0.33	0.49		0.32	0.45		7.56	8.02	9.20	1.27	1.27 [24]
14	0.27	0.35	−0.23	0.24	0.32	−0.20	6.40	7.20	7.59 [24]	1.28	1.27 [24]
	0.27	0.34		0.23	0.31		6.55	7.47	7.59	1.27	1.30
15	0.29	0.36	−0.21	0.25	0.33	−0.17	3.46	3.8	3.5 [25]	1.27	1.28 [25]
	0.29	0.36		0.25	0.33		3.46	3.8	3.5	1.28	1.28
	0.34	0.45		0.31	0.44		3.93	4.42	4.4	1.26	1.28
16	0.45	0.55	−	0.45	0.53		10.95	11.48	12.0 [26]	1.29	—

The second row of each compound contains data for the second NO group in the molecule.

[a] In different non-aqueous solutions.
[b] Compounds prepared in the present work.
[c] Similar compounds.
[d] Results of the present work.

Unfortunately, there are no experimental spin densities for planar nitronyl nitroxides (**8–10**) and iminyl nitroxides (**12,13**) to enable the comparison with the calculated results. The calculated iminyl nitroxides spin densities are mostly distributed on the N=C–N–O$^{\bullet}$ fragment (see Table 1). The smaller values of the spin densities on the O–N=C–N–O$^{\bullet}$ fragment in **8**, **9** and **10** can be rationalized by the additional delocalization of unpaired electron on the carbons of the adjacent ring (0.02–0.05 μ_B).

Different substituents such as pyridine, Cl, NO$_2$ and S slightly change the spin densities distribution on the O–N=C–N–O$^{\bullet}$ fragment of the nitroxide radicals and NO distances (second row of each compound in Table 1). The changes of the calculated spin densities on the O–N=C–N–O$^{\bullet}$ fragment of different substituted nitronyl nitroxide radicals are also given in Ref. [8]. Intramolecular hydrogen bond NO–HO in **5** signifi-

cantly affects the spin density distribution on the O–N=C–N–O$^{\bullet}$ fragment: 0.27 μ_B on nitrogen and 0.23 μ_B on the oxygen atom that is participating in the hydrogen bond compared with 0.28 μ_B on nitrogen and 0.42 μ_B on the other oxygen atom and N–O distances. The spin density on the α-carbon atom is −0.195 μ_B. Similar changes were found for (**8**). This effect has also been observed in PND studies on O–N=C–N–O$^{\bullet}$ fragment; 0.203 μ_B on the N atom and 0.242 μ_B on the O atom linked by CH–ON intermolecular hydrogen bond compared with 0.225 μ_B on the N atom, 0.278 μ_B on the other O atom and −0.071 μ_B on the C atom [29].

The smaller values of the spin density at the NO group connected to the phenyl ring (**15**) in comparison with (**16**) may be explained by the relatively larger corresponding unpaired electron delocalization on the carbon atom in the 2,4,6 positions of the phenyl ring. The spin density on the carbon atoms at the 2,4,6

positions of the phenyl has been calculated to be 0.14–0.16 μ_B, while the spin densities on the corresponding carbon atoms in the other molecules are in a range of 0.01–0.05 μ_B.

The calculated spin densities are almost independent of the torsion angle between NO$^\bullet$ and the phenyl rings. The experimental data confirm this conclusion [27–29].

The given experimental nitrogen hfcc's have been measured in different non-aqueous solvents at room temperature. The experimental results for nitronyl nitroxides radicals with one unpaired electron (**1–6**, **11** and **14**) are in the range of 7.0–7.81 G, for planar nitronyl nitroxide radicals (**8–10**) are in the range 4.1–4.38 G and for nitronyl nitroxides radicals with two unpaired electrons (**7** and **15**) are in the range of 3.5–3.8 G. The experimental data for iminyl nitroxides radicals (**12** and **13**) were found to be 8.9–9.2 G for the nitrogen nucleous in the NO group and 4.28–4.5 G for the other nitrogen nucleous.

All the UB3LYP calculated hfcc's of nitronyl nitroxides radicals with one unpaired electron are in a range of 5.97–6.7 G and the corresponding UB1LYP calculated hfcc's are in a range of 6.7–7.47 G. UBLYP hfcc's calculations underestimate the experimental and UB3LYP results by more than 1 G. According to these data, one may conclude that UB1LYP provides hfcc's for nitronyl nitroxides radicals closer to the experimental ones (7.0–7.81 G).

The hfcc's calculations for the diradicals (**7,9,15**) were performed for their triplet states, i.e. ferromagnetic coupling between radical centers was assumed. Experimentally, it was observed only for (**15**) [25], as the intramolecular distances between radicals centers for (**7**) are too large for coupling ($>10\,\text{Å}$) [20] and unfortunately there are no experimental data for (**9**).

The nitrogen hfcc's of planar nitronyl nitroxides radicals with one unpaired electron (**8** and **10**) have been calculated to be 3.59–3.74 (UB3LYP) and 4.15–4.27 (UB1LYP). UB1LYP results for planar nitronyl nitroxides radicals are closer to the experimental data (4.1–4.38 G).

The nitrogen hfcc of planar nitronyl nitroxides radical (**9**) with two unpaired electrons was calculated to be 1.73 G (UB3LYP) and 2.06 G (UB1LYP).

The nitrogen hfcc's of iminyl nitroxides radical have been calculated to be 5.26–5.32 (UB3LYP), 5.48–5.76 (UB1LYP) and 7.56–7.87 (UB3LYP), 7.35–8.02 (UB1LYP). Both UB3LYP and UB1LYP results for iminyl nitroxides are significantly different from the experimental data (4.28–4.5 and 8.9–9.2 G correspondingly).

UBLYP calculations of the hfcc's for the presented compounds show a decrease up to 2 G in comparison with the experimental and UB3LYP calculated results. The decrease of the calculated hfcc's for **8**, **9** and **10** in comparison with the other nitronyl nitroxides radicals

may be attributed to the additional unpaired electron delocalization on the adjacent rings. Replacing an H atom in the ortho position of the phenyl ring by Cl (**4**), OH (**5**), (**8**), and COOH (**14**) leads to the slight increase of neighboring nitrogen hfcc. This effect was experimentally observed only for a similar compound to **5** [19]. Replacing the phenyl ring by pyridine (**6**) and thiophene (**11**) ring leads to the slight increase of neighboring nitrogen hfcc as well. The absence of slight increase of the hfcc's in the experiments might be explained by the low resolution of the bands in EPR measurements. It is therefore possible to conclude that the different surroundings of the radical centers may slightly change the nitrogen hfcc's. The relatively large nitrogen hfcc of **16** in comparison with the other compounds may be explained by the larger spin density on the NO radical center.

The nitrogen hfcc's obtained by the UB1LYP/6-31 G(d) calculations shown in the present work is in a better agreement than those obtained by the use of UB3LYP calculation with the specially developed EPR II basis set [17] for similar nitronyl nitroxide radicals.

4. Conclusions

UB3LYP and UB1LYP with 6-31G(d) calculated nitronyl nitroxides radicals hfcc's are in a very good agreement with the experimental results. UB1LYP with 6-31G(d) basis set sometimes slightly overestimates hfcc's for nitronyl nitroxides radicals, but in most cases it provides better results than UB3LYP.

UBLYP and UB3LYP calculated spin densities for the presented radicals are almost identical. The presented results show that the UB3LYP and UB1LYP methods with a 6-31G(d) basis set of Gaussian 98 can be used for the predictions of molecular magnetic properties.

Acknowledgments

References

[1] H.M. McConnell, J. Chem. Phys. 39 (1963) 1910.
[2] M. Tamura, Y. Nakazava, K. Nozava, D. Shiomi, Y. Hosokushi, M. Ishikava, M. Takahashi, M. Kinoshita, Chem. Phys. Lett. 186 (1991) 401.

[3] A.J. Banister, N. Bricklebank, I. Lavender, J.M. Rawson, C.I. Gregory, B.K. Tanner, W. Clegg, M.R.G. Elsegood, F. Palacio, Chem. Int. Ed. Engl. 21 (1996) 2533–2535.

[4] J.S. Miller, A.J. Epstein, Angew. Chem. Int. Ed. Engl. 33 (1994) 385–415.

[5] M. Deumal, J. Cirujeda, J. Veciana, J.J. Novoa, Adv. Mater. 10 (1998) 1461.

[6] M. Deumal, J. Cirujeda, J. Veciana, J.J. Novoa, Chem. Eur. J. 5 (1999) 1631.

[7] P. Turek, K. Nozava, D. Shiomi, K. Awaga, T. Inabe, Y. Maruyama, M. Kinoshita, Chem. Phys. Lett. 180 (1991) 327–331.

[8] M. Deumal, P. Lafuente, F. Mota, J.J. Novoa, Synth. Metals 122 (2001) 477–483.

[9] J. Foresman, E. Frish, Exploring Chemistry, Gaussian Inc., Pittsburg, USA, 1996.

[10] A. Beck, J. Chem. Phys. 98 (1993) 1372.

[11] A. Beck, Phys. Rev. A 38 (1988) 3098.

[12] C. Lee, W. Yang, R. Parr, Phys. Rev. B 37 (1988) 785.

[13] O. Gunnarson, B.I. Lundqist, Phys. Rev. B 13 (1976) 4274.

[14] A. Beck, J. Chem. Phys. 98 (1993) 5648.

[15] J.P. Perdew, M. Ernzerhof, K. Burke, J. Chem. Phys. 105 (1996) 9982.

[16] W. Weltner Jr., Magnetic Atoms and Molecules, Dover, New York, 1989.

[17] J. Cirujeda, J. Vidal-Gansedo, O. Jurgens, F. Mota, J.J. Novoa, C. Rovira, J. Veciana, J. Am. Chem. Soc. 122 (46) (2000) 11393–11405.

[18] E.F. Ulman, J.H. Osiecky, D.G.B. Boocock, R. Darcy, J. Am. Chem. Soc. 94 (20) (1974) 7049–7059.

[19] O. Jurgens, J. Cirujeda, M. Mas, I. Mata, A. Cabrero, J. Vidal-Cancedo, C. Rovira, E. Molins, J. Veciana, J. Mater. Chem. 7 (1997) 1723–1730.

[20] R. Ziessel, G. Ulrich, R.C. Lawson, L. Echegoyen, J. Mater. Chem. 9 (1999) 1435–1438.

[21] D. Shiomi, K. Sato, T. Takui, K. Itoh, M. Tamura, Y. Nishio, K. Kajita, M. Nakagawa, T. Ishida, T. Nogami, Mol. Cryst. Liq. Cryst. 335 (1999) 359–369.

[22] Y. Kusaba, M. Tamura, Y. Hosokoshi, M. Kinoshita, H. Sawa, R. Kato, H. Kobayashi, J. Mater. Chem. 7 (8) (1997) 1377–1382.

[23] T. Akita, Y. Mazaki, K. Kobayashi, N. Koga, H. Iwamura, J. Org. Chem. 60 (1995) 2092–2098.

[24] C. Stroch, F.M. Romero, N. Kyrisakas, L. Catala, Ph. Turek, R. Ziessel, J. Mater. Chem. 9 (1999) 875–882.

[25] K. Inoe, H. Iwamura, Angew. Chem. Int. Ed. Engl. 34 (8) (1995) 927–928.

[26] A.G. Davies, J.A-A. Hawari, M. Whitefield, Polyhedron Lett. 20 (1983) 4465–4468.

[27] A. Zheludev, V. Barone, M. Bonnet, B. Delley, A. Grand, E. Ressouche, P. Ray, R. Subra, J. Schweizer, J. Am. Chem. Soc. 116 (1994) 2019–2027.

[28] F.M. Romero, R. Ziessel, M. Bonnet, Y. Pontillion, E. Ressouche, J. Schweizer, B. Delley, A. Grand, C. Paulsen, J. Am. Chem. Soc. 121 (41) (1999) 9659–9667.

[29] Y. Pontillion, A. Caneschi, D. Gatteschi, A. Grand, E. Ressouche, R. Sesoli, J. Schweizer, Chem. Eur. J. 5 (12) (1999) 3616–3624.

[30] H. Heise, F.H. Kohler, F. Mota, J.J. Novoa, J. Veciana, J. Am. Chem. Soc. 122 (7) (2000) 1298–1309.

[31] S. Yamanaka, T. Kawakami, S. Yamada, H. Nagao, M. Nakano, K. Yamaguchi, Chem. Phys. Lett. 240 (1995) 268–277.